NASA/TM-20210018297

Microwave Photoelasticity: Exploiting Multiple Resonances To Measure Stress Changes Within Yttria-Partially-Stabilized Zirconia

Seth W. Waldstein and Peter J. Schemmel
Glenn Research Center, Cleveland, Ohio

October 2021

NASA STI Program . . . in Profile

Since its founding, NASA has been dedicated to the advancement of aeronautics and space science. The NASA Scientific and Technical Information (STI) Program plays a key part in helping NASA maintain this important role.

The NASA STI Program operates under the auspices of the Agency Chief Information Officer. It collects, organizes, provides for archiving, and disseminates NASA's STI. The NASA STI Program provides access to the NASA Technical Report Server—Registered (NTRS Reg) and NASA Technical Report Server—Public (NTRS) thus providing one of the largest collections of aeronautical and space science STI in the world. Results are published in both non-NASA channels and by NASA in the NASA STI Report Series, which includes the following report types:

- TECHNICAL PUBLICATION. Reports of completed research or a major significant phase of research that present the results of NASA programs and include extensive data or theoretical analysis. Includes compilations of significant scientific and technical data and information deemed to be of continuing reference value. NASA counter-part of peer-reviewed formal professional papers, but has less stringent limitations on manuscript length and extent of graphic presentations.

- TECHNICAL MEMORANDUM. Scientific and technical findings that are preliminary or of specialized interest, e.g., "quick-release" reports, working papers, and bibliographies that contain minimal annotation. Does not contain extensive analysis.

- CONTRACTOR REPORT. Scientific and technical findings by NASA-sponsored contractors and grantees.

- CONFERENCE PUBLICATION. Collected papers from scientific and technical conferences, symposia, seminars, or other meetings sponsored or co-sponsored by NASA.

- SPECIAL PUBLICATION. Scientific, technical, or historical information from NASA programs, projects, and missions, often concerned with subjects having substantial public interest.

- TECHNICAL TRANSLATION. English-language translations of foreign scientific and technical material pertinent to NASA's mission.

For more information about the NASA STI program, see the following:

- Access the NASA STI program home page at http://www.sti.nasa.gov

- E-mail your question to help@sti.nasa.gov

- Fax your question to the NASA STI Information Desk at 757-864-6500

- Telephone the NASA STI Information Desk at 757-864-9658

- Write to:
  NASA STI Program
  Mail Stop 148
  NASA Langley Research Center
  Hampton, VA 23681-2199

NASA/TM-20210018297

Microwave Photoelasticity: Exploiting Multiple Resonances To Measure Stress Changes Within Yttria-Partially-Stabilized Zirconia

Seth W. Waldstein and Peter J. Schemmel
Glenn Research Center, Cleveland, Ohio

National Aeronautics and
Space Administration

Glenn Research Center
Cleveland, Ohio 44135

October 2021

Acknowledgments

This work is supported by the NASA Aeronautics Research Mission Directorate, Transformational Tools and Technologies Project.

This work was sponsored by the
Transformative Aeronautics Concepts Program.

Level of Review: This material has been technically reviewed by technical management.

Available from

NASA STI Program
Mail Stop 148
NASA Langley Research Center
Hampton, VA 23681-2199

National Technical Information Service
5285 Port Royal Road
Springfield, VA 22161
703-605-6000

This report is available in electronic form at http://www.sti.nasa.gov/ and http://ntrs.nasa.gov/

Microwave Photoelasticity: Exploiting Multiple Resonances To Measure Stress Changes Within Yttria-Partially-Stabilized Zirconia

Seth W. Waldstein and Peter J. Schemmel
National Aeronautics and Space Administration
Glenn Research Center
Cleveland, Ohio 44135

Abstract

The NASA Glenn Research Center is developing nondestructive testing (NDT) methods to enable the measurement of stresses embedded in optically opaque materials using microwave radiation in a free-space quasi-optical system. This methodology tracks microwave resonances observed in reflected scattering parameters extracted from materials under load. In this paper, we report the successful measurement of the stress-optic coefficient of bulk yttria-partially-stabilized zirconia (YTZP) ceramic of $C = 1.42\times10^{-4} \pm 6.65\times10^{-6}$ (1/GPa), across W-Band (80 to 100 GHz), and determined that this result is independent of sample thickness. The primary goal of this research is to establish a methodology to quantify and assess the life expectancy of ceramic thermal and environmental barrier coating (TBCs/EBCs). Bulk YTZP samples can undergo multiple resonances within a contiguous measurement bandwidth, each corresponding to an integer multiple wave number α. This allows for the acquisition and analysis of multiple stress measurement points within a single sample. As an additional benefit, one can approximate the refractive index of YTZP across a wide bandwidth by observing multiple resonances produced by a set of samples with varying thicknesses. Using this approach, the refractive index of bulk YTZP was found to be $n = 5.80 \pm 0.043$ across the 85 to 115 GHz frequency band.

1.0 Introduction and Motivation

Thermal barrier coatings (TBC) help prevent failures of critical gas-turbine engine components exposed to high temperatures or pressures. Yttria-partially-stabilized zirconia (YTZP), a common TBC material, is a tetragonal phase of Zirconium Dioxide ($Zr0_2$) produced by calcining zirconium compounds between 1170 and 2370 °C (Ref. 1). The addition of yttrium oxide (Y_2O_3, yttria) produces a stabilized tetragonal formation at room temperature. In a typical TBC system, YTZP comprises the topcoat of a four-layer stack which also includes a super alloy substrate, thermally grown oxide (TGO) and bond layer. Deposition of the YTZP through electron beam physical vapor deposition (EBPVD) or air plasma spray (APS) produces varying structural morphologies and results in differing failure mechanisms (Refs. 2 and 3). Spallation of the ceramic topcoat is the primary cause for failure in both EBPVD and APS coatings, which may result in eventual engine failure (Ref. 4).

Currently, NASA Glenn Research Center is developing a methodology to better understand stress embedded within TBCs. Analysis on the cost savings attained through mean-lifetime estimations using nondestructive testing (NDT) of TBCs shows the value in techniques that can accurately determine the condition of these critical parts (Ref. 5). Techniques are currently being investigated to determine

qualitative metrics that correlate in-situ stress with the life expectancy of a TBC. The development of qualitative relationships between in-situ stress and expected remaining life would enable the removal of sub-optimal components from assembly, preventing part failure and address a major challenge in TBC development (Ref. 5).

Destructive testing methods are prohibitively expensive and not intended for in-situ component assessment. Several alternative NDT methods used to inspect TBC properties have been previously described in Reference 6, each with their own advantages and limitations. NDT for measurement of direct stress-optic coefficients (C) in ceramic TBCs have been previously presented showing that YTZP exhibits stress induced birefringence in the linear elastic regime when illuminated with GHZ radiation (Ref. 6).

It is important to develop innovative new NDT methods that complement existing techniques. In this paper we demonstrate - for the first time - a measurement of a direct stress-optic coefficient in bulk YTZP across the 80 to 100 GHz bandwidth utilizing a resonant wavelength approach. The resonant wavelength approach is powerful in that a single sample can be analyzed at multiple resonances, dependent on material properties and acquisition bandwidth. This allows for the collection of multiple data points for analysis of stress, and, in addition, can collectively represent an approximation of the material properties across a specific bandwidth. This approach is used to approximate the refractive index (n) of bulk YTZP across the 85 to 115 GHz bandwidth. This paper is part of a series, following "Microwave Photoelasticity: A Resonant Wavelength Approach Applied to PEEK Polymer," which describes this innovative measurement technique applied to materials of interest to the aerospace engineering community (Ref. 7).

Section 2.0 of this papers details the theoretical methodology behind the resonant wavelength approach. Section 3.0 presents the experimental setup for measurement acquisition along with procedural details. Measured results are then summarized in section 4.0, followed by a results discussion in section 5.0, and then the paper concludes in section 6.0.

2.0 Theoretical Methodology

2.1 Determining Stress-Optic Coefficients Using S-Parameters

Microwave Photoelasticity (MP) analysis is conducted by observing scattering parameters with a quasi-optical free space instrument using a method previously described in Reference 8. The technique monitors a series of frequency (or wavelength) dependent troughs, in the measured reflection S-parameters, due to destructive interference between microwave signals within the sample. Changes to the resonant frequency are correlated to changes in stress, via the stress-optic law.

The specific method used in this paper is derived from the Fresnel Equation (1) which relates the refractive index n to the free-space wavelength λ_0 (or frequency f_0),

$$n = \frac{\alpha}{2*d}\lambda_0 = \frac{\alpha}{2*d}\cdot\frac{c}{f_0} \tag{1}$$

where α is an unknown integer number corresponding to the number of half wavelengths in the sample, c being the speed of light in a vacuum, and d is sample thickness (Ref. 7). Figure 1 presents a graphical representation of a wave with wavelengths equal to integer multiples of the sample thickness.

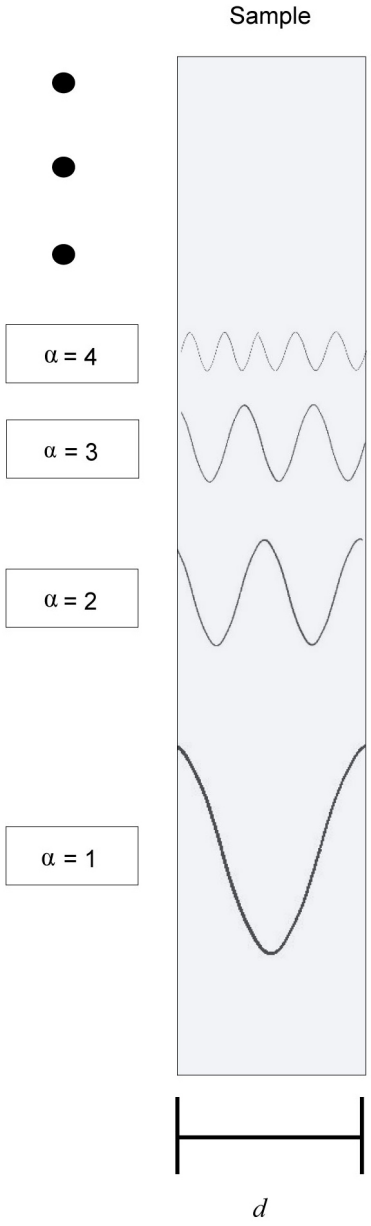

Figure 1.—A graphic representation of α as integer multiples of half-wavelengths traveling through a sample.

The stress-optic law Equation (2) describes the linear relationship between refractive index and stress with the direct stress-optic coefficient *C*, and principal stress σ in the case of a uniaxial load such that the transverse stress is approximately zero (Ref. 6).

$$\Delta n = C\Delta\sigma \tag{2}$$

Replacing Δσ with a common form of stress used for typical tensile testing specimens with rectangular cross-sections, $\frac{\Delta F}{w * d}$, where *F* = force, results in a relation between refractive index, stress and *C*.

$$\Delta n = C\frac{\Delta F}{w * d} \tag{3}$$

Equating (1) and (3) allows for the representation of a change in resonant frequency as the product of the material's stress-optic coefficient, the unknown integer α, and material width, resulting in Equation (4).

$$\Delta f_0 = \left(\frac{c * \alpha * w}{2 * C}\right) * \frac{1}{\Delta F} \tag{4}$$

When plotting resonant frequency versus applied load, the resulting slope will depend on material properties *C*, α and sample width (provided that the stress may be described as the force over cross-sectional area). A material's stress-optic coefficient is independent of sample thickness so this resonant frequency method should extract the same *C* for any sample thickness.

2.2 Determining Stress-Optic Coefficients Using Multiple Resonant Frequencies

The resonant wavelength approach can be used to analyses multiple resonant α's at the same time on a single sample. This allows for the collection of multiple data points and an approximation of the material properties across a bandwidth.

The α of each resonance is first determined with Equation (1), using a refractive index number acquired from a known method, such as the Nicholson-Ross-Weir (NRW) method, and then solving for α. This α term is then rounded to the nearest integer and then plugged back into Equation (1) to solve for refractive index. Stitching together the analysis of multiple peaks of sequential α's of multiple sample thicknesses gives the material's general refractive index across a set bandwidth.

3.0 Measurement Setup

The experimental setup, seen in Figure 2, consists of a Vector Network Analyzer (VNA) (Anritsu MS4647B with 3743A mmW frequency extension modules) operating from 70 KHz to 120 GHz, connected to two W-band circular horn antennas. The horn antennas transmit and receive a linearly polarized diverging beam while the two polytetrafluoroethylene (PTFE) lenses focus the beam onto the center of the sample with a spot size of ≈10 mm. A Deben MT2000 tensile stage holds the sample at the calibration plane and applies a variable uniaxial load in the vertical direction. The measurement methodology was such that the stress vector is perpendicular to the microwave propagation axis.

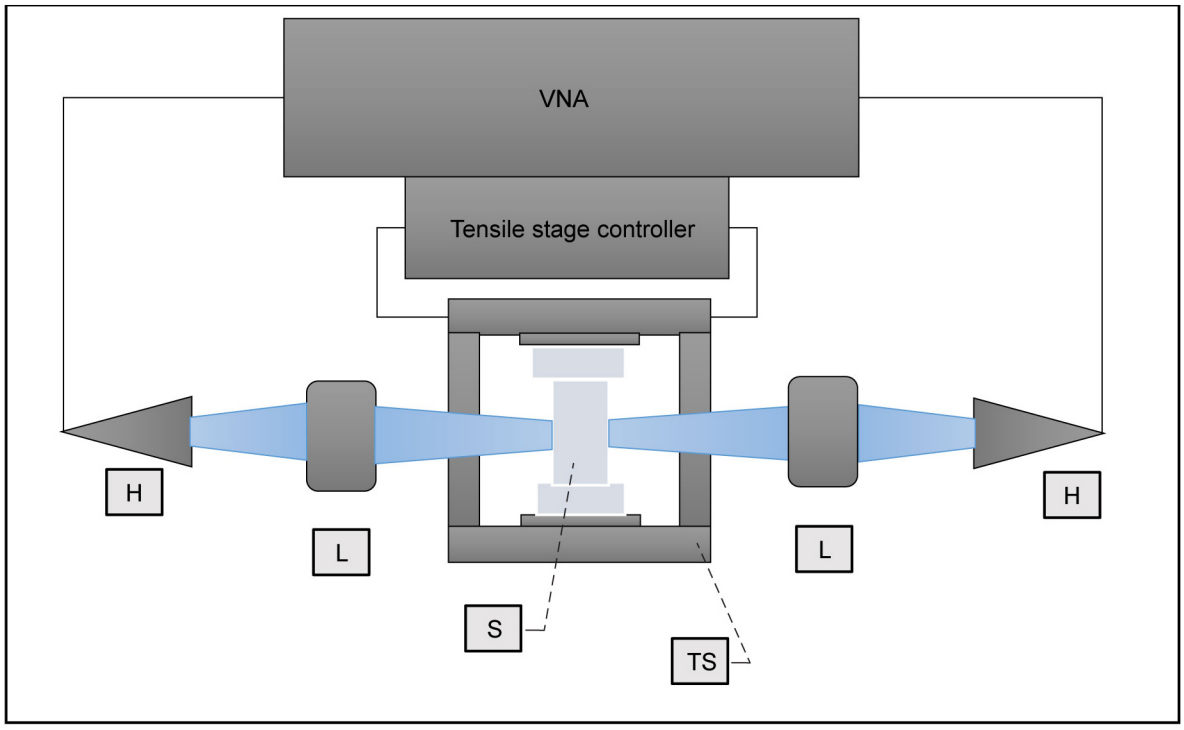

Figure 2.—Schematic of experiment setup used to measure direct stress-optic coefficient in YTZP. With W-band Horn (H), PTFE Lens (L), specimen (S), tensile stage (TS) along with VNA and tensile stage controller.

Before the collection of data, the VNA was calibrated using a standard thru-reflect-match (TRM) procedure across the bandwidth of 80 to 120 GHz at a 10.0 MHz step size. The testing configuration, seen in Figure 3, was such that the calibration plane of the 2-port system bisects the sample when mounted in the tensile stage. In addition to calibration, VNA time gating is used to minimize artifacts induced by the measurement setup. A time gating span of 255 ps was used with a relative post-calibration position of –30 to 225 ps.

Bulk YTZP ceramic samples were sintered and fired into dog bone shapes, all cut to the same width and length dimension with variable thicknesses of 1.5, 2.0, and 3.0 mm. Information on the YTZP sample fabrication and material properties have been previously reported in Reference 5. The samples were secured in the tensile stage using steel dowel pins, rounded shoulders screws, and plastic shims to protect the YTZP from cracking due to the pressure of the tensile stage's metal brackets.

An initialization of each sample was performed by applying stress up to 1,800 N at an extension rate of 0.5 mm/s, and then reversing back down to 10 N. The test procedure includes first, increasing to a predetermined stress level and then acquiring a set of S-parameter measurements while maintaining a constant tensile load. The tensile stage is then adjusted to the next stress level in preparation of the following RF measurement. The full measurement set on a single sample includes three cycles of loading and unloading from 10 to 1,800 N while taking 10 measurements, in both the increasing and decreasing loading directions. Measurements were conducted using three individual samples of each sample thickness (1.5, 2.0, and 3.0 mm).

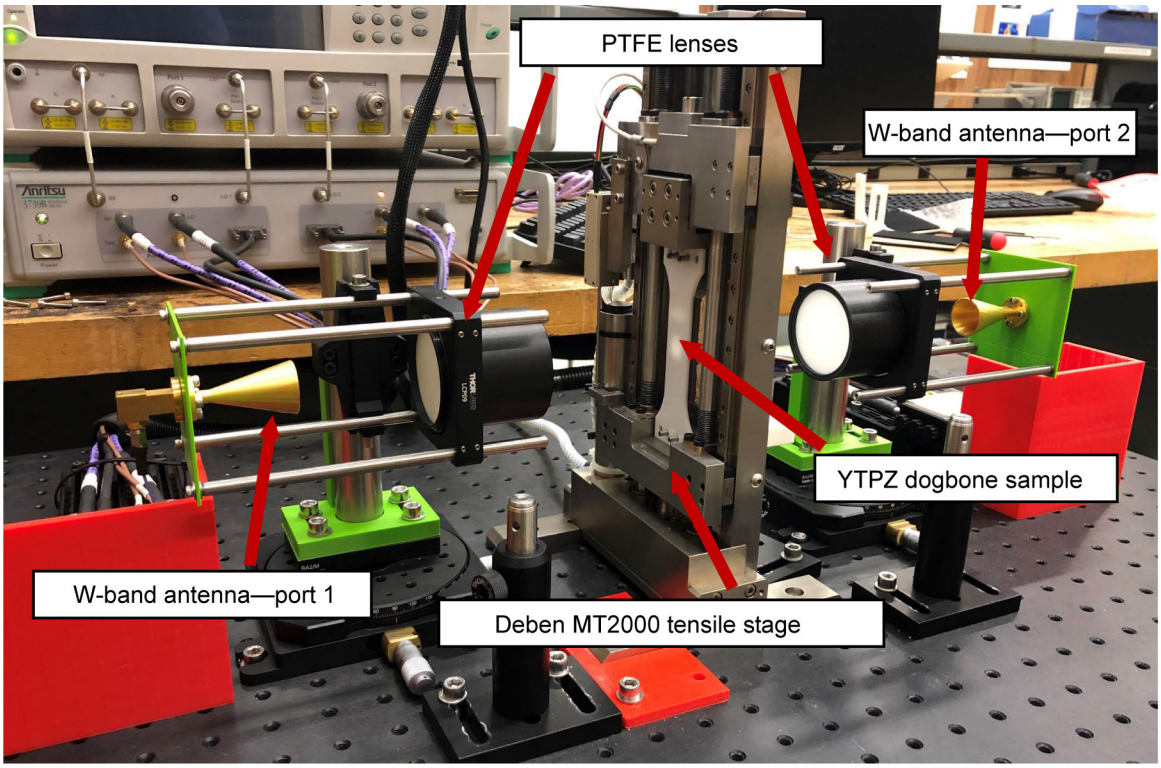

Figure 3.—Free space measurement experimental setup consisting of horn antennas, PTFE lenses, tensile stage, and YTZP dog bone samples.

The measured S-parameters, specifically the input and output reflection coefficient, were extracted to determine the resonant frequencies of each sample. A quadric fit (dashed black line) is first applied to the measured S-parameters data and used for approximation of the resonant frequency. The red dots in Figure 4 represent resonant frequency analysis points extracted from the S_{11} and S_{22} of a 3.0 mm thick sample of YTZP. In this example, (Figure 4) the reflection coefficient measured from port 2 of the VNA has a resonant frequency of ≈95.3 GHz, corresponding to an α of 11.

4.0 YTZP Results

4.1 Extraction of Stress-Optic Coefficient of YTZP

This section determines the stress-optic coefficient of bulk YTZP and demonstrates that C is independent of sample thickness. The successful extraction of bulk YTZP's stress-optic coefficient with accurate repeatability has been demonstrated across sample thickness. A resonant frequency offset can be observed in Figure 5(a) which are $\Delta f_0/\Delta F$ (GHz/N) measurements of the three separate 2.0 mm thick samples of bulk YTZP before offset correction. This offset has been observed before and shown to be due to uncertainty in the measured thickness of each specimen (Ref. 4). Figure 5(b) presents the same data after the offset correction. Accuracy across all 2.0 mm samples can be observed through the close alignment of these three slopes after offset correction.

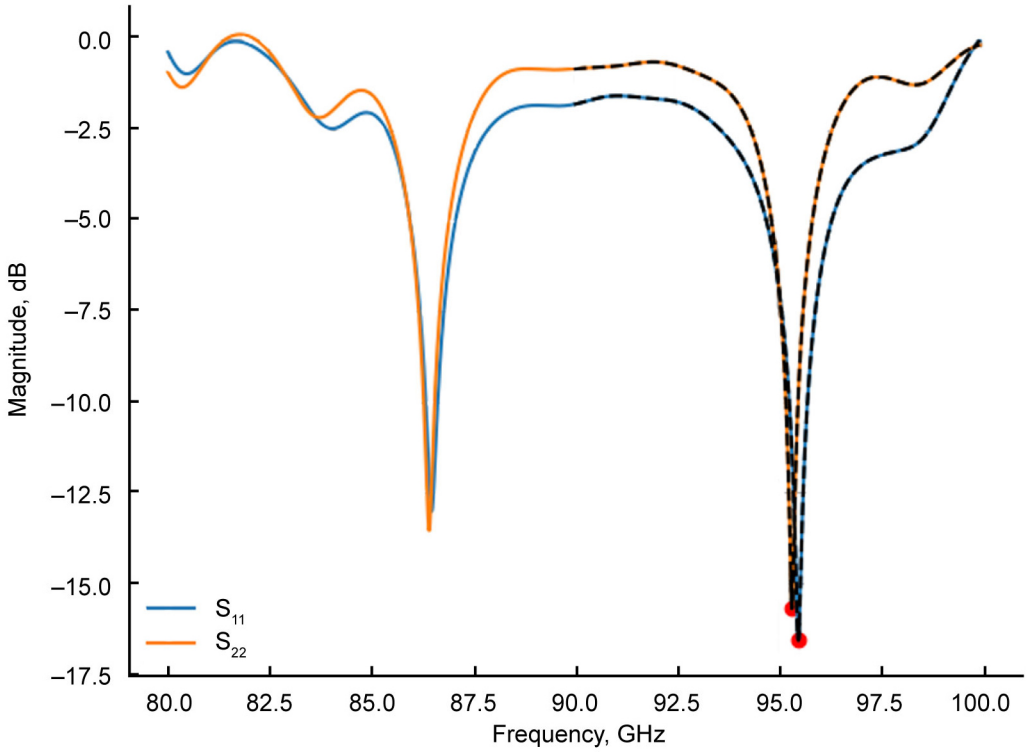

Figure 4.—Plot of input and output reflection coefficient for a 3 mm bulk YTZP.

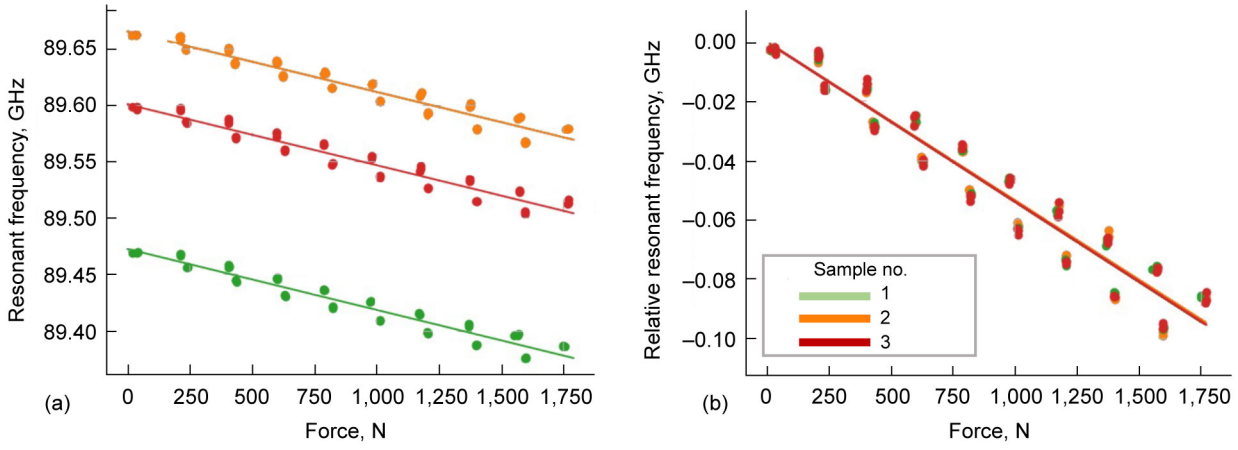

Figure 5.—Plots of (a) Resonant frequency vs. force (b) Relative resonant frequency vs. force for three various YTZP samples of 2 mm thickness.

Figure 6 presents a plot of relative resonant frequency (GHz) versus stress (Mpa) for a 3.0, 2.0, and 1.5 mm samples. An average slope of relative resonant frequency versus stress after normalization is measured at –2.173 ± 0.047 (GHz/Mpa) across sample thicknesses. Accuracy of this method is observed through the error in the alignment of the slopes being < 1 percent. Hysteresis is observed in the measurements shown in Figure 5 as the separation between forward (below the trend line) and reverse (above trend line) loading states.

Figure 6 clearly demonstrates that hysteresis increases as sample thickness decreases. Further research is required to understand the physics and material properties behind this result, and we encourage the engagement from the wider nondestructive testing community.

Results, summarized in Table 1, presents resonant frequency under no-load of each sample thickness, the ratio of the change in resonant wavelength versus force, and the extracted direct stress-optic coefficient measurements normalized for sample thickness. This data shows that YTZP's direct stress-optic coefficient can be accurately measured using the resonant wavelength approach, and that this approach can be employed independent of sample thickness. An average value of $C = 1.42\times10^{-4} \pm 6.65\times10^{-6}$ (1/GPa) was extracted for the direct stress-optic coefficient of YTZP, across the 80 to 100 GHz bandwidth.

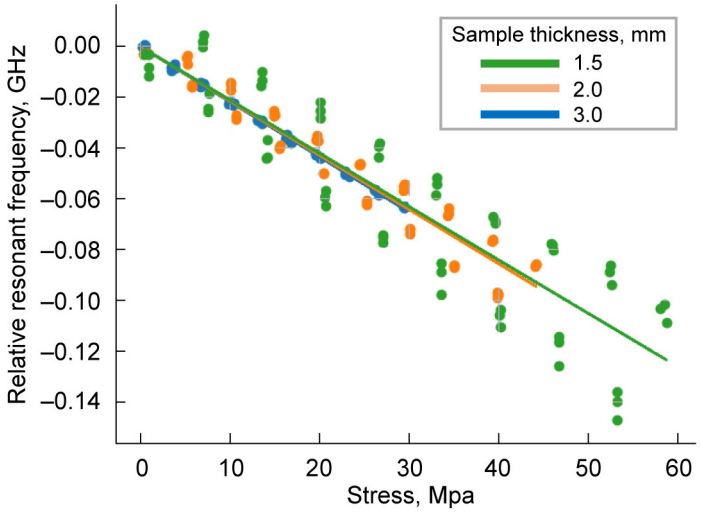

Figure 6.—Plots of relative resonant frequency vs. stress for three YTZP samples of thicknesses 1.5, 2.0, and 3.0 mm.

TABLE 1.—RESULTS SUMMARY WITH RESONANT FREQUENCY $_{(no\ load)}$ AND DIRECT STRESS OPTIC COEFFICIENT OF YTZP

Sample thickness, mm	Resonant frequency $_{no\ load}$, GHz	$\Delta\lambda_0/\Delta F$, mm/N	C, 1/GPa
$1.5_{\alpha=5}$	≈84.60 ± 0.063	$3.01\times10^{-6} \pm 5.83\times10^{-8}$	$1.51\times10^{-4} \pm 2.91\times10^{-6}$
$2.0_{\alpha=7}$	≈89.54 ± 0.065	$2.01\times10^{-6} \pm 1.06\times10^{-8}$	$1.41\times10^{-4} \pm 7.44\times10^{-7}$
$3.0_{\alpha=11}$	≈95.31 ± 0.060	$1.22\times10^{-6} \pm 2.42\times10^{-8}$	$1.34\times10^{-4} \pm 2.66\times10^{-6}$

4.2 Extraction of $\frac{\Delta\lambda_0/\alpha^\circ}{\Delta F}$ for Different α

Seen through Equation (4), changes in resonant frequency versus applied force are related by α. This means analysis can be performed on any α within a measurement bandwidth, which should result in the same relative slope of $\Delta\lambda_0/\Delta F$ after normalization of the α term. Figure 7 presents a measurement window from 80.0 to 100.0 GHz which contains two separate resonant frequencies from a 3.0 mm YTZP sample corresponding to an (a) α = 10 between 85.0 to 87.5 GHz and (b) α = 11 between 93.0 to 97.0 GHz.

These two points can be independently analyzed, normalized for α, and confirmed against each other for accuracy determination. Figure 8 presents plots of the relative resonant frequency versus force after normalization of α for (a) α = 10 between 85.0 to 87.5 GHz and (b) α = 11 between 93.0 to 97.0 GHz. Table 2 presents the results of this analysis showing the slope of change in resonant frequency versus applied force after normalization of alpha being closely correlated. The accuracy of these results are shown by the close similarity of the extracted slopes of change in resonant frequency versus applied force for both the analysis of α = 10 and α = 11.

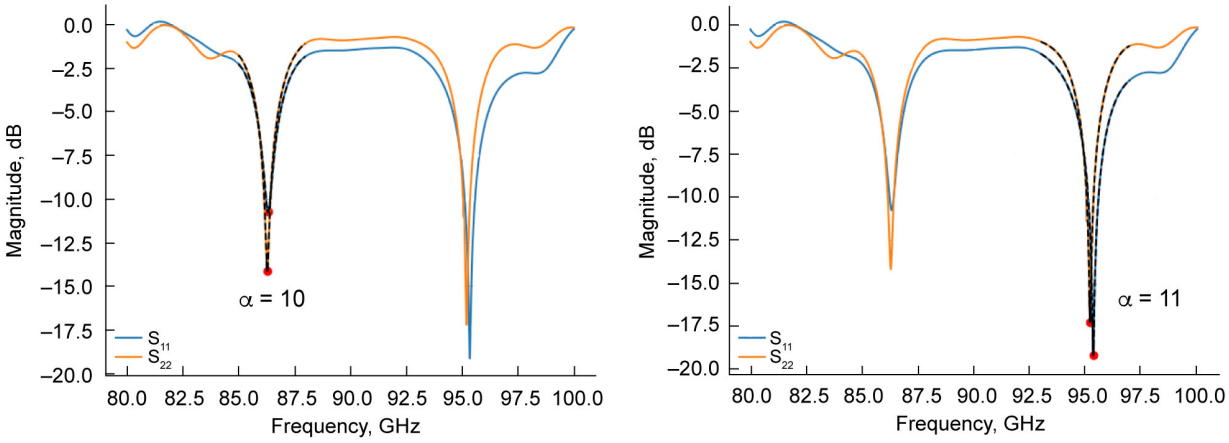

Figure 7.—Plots of input and output reflection coefficient for a 3 mm bulk YTPZ samples showing analysis window for (a) α = 11 between 85.0 to 87.5 GHz and (b) α = 11 between 93.0 to 97.0 GHz.

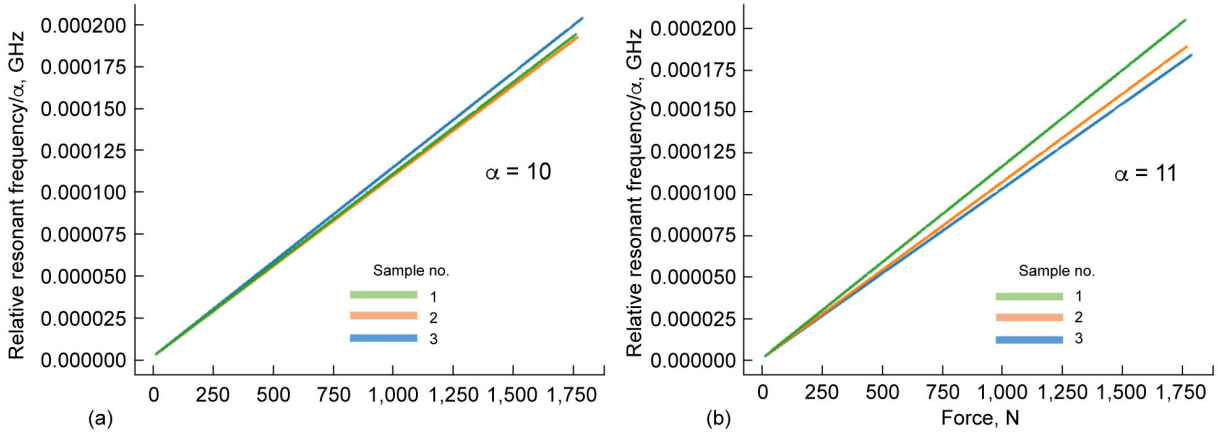

Figure 8.—Plots of λ_0/α = 11 vs. applied force for 3.0 mm samples of bulk YTZP corresponding to (a) α = 10 found between 85.0 to 87.5 GHz and (b) α = 11 found between 93.0 to 97.0 GHz.

TABLE 2.—RESULTS OF CHANGE IN RESONANT FREQUENCY VERSUS APPLIED FORCE AFTER NORMALIZATION OF α

	$\frac{\Delta\lambda_0/\alpha^\circ}{\Delta F}$	
Sample number	α = 10	α = 11
S_1	1.14×10^{-7}	1.01×10^{-7}
S_2	1.09×10^{-7}	1.05×10^{-7}
S_3	1.10×10^{-7}	1.14×10^{-7}

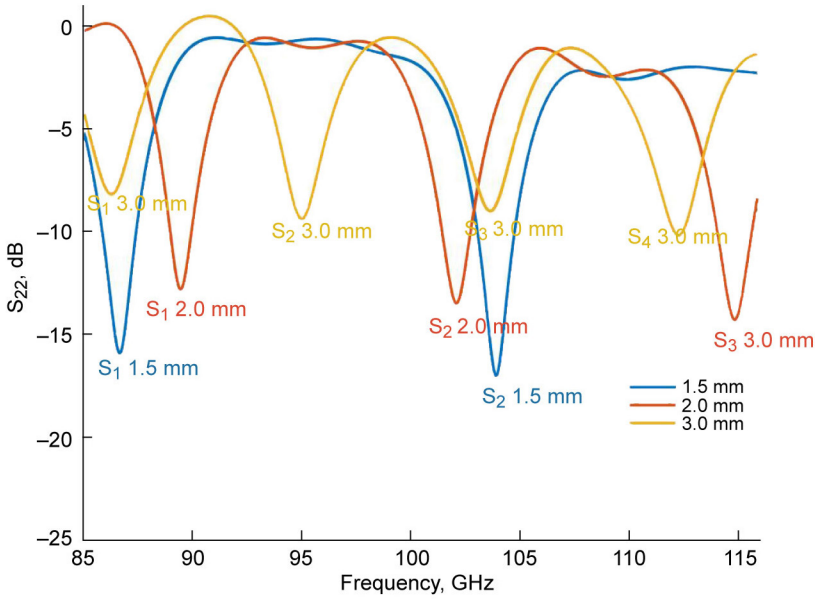

Figure 9.—Overlay of S_{22} measurements from the VNA of bulk YTZP of thicknesses 1.5, 2.0, and 3.0 mm across the bandwidth of 85 to 120 GHz.

4.3 Confirmation of α and Extraction of YTZP Refractive Index

Each resonant wavelength point, seen across the bandwidth, can be used for extraction of a material refractive index. An overlay of the S_{22} for each of the three samples thicknesses is shown in Figure 9 across the 85 to 120 GHz bandwidth. Within this band, nine resonant frequency points can be analyzed from these specific sample widths. Additional points could be acquired for this analysis through the addition of more sample width variation.

Through manipulation of Equation (1) and by using an approximate refractive index value obtained from an alternative method, α can be approximated and rounded to the nearest integer. Through rearranging Equation (1) and plugging in the rounded α allows for the calculation of refractive index. Table 3 presents a results summary of the nine resonant frequency points along with their corresponding λ_0, α, and n.

Figure 10 presents a plot of refractive index measurements of YTZP extracted from the resonant wavelength approach, along with the refractive index of YTZP extracted using the NRW method with μ = 1 (Ref. 9).

An average value of $n = 5.80 \pm 0.043$ for bulk YTZP has been extracted using the resonant wavelength method for a bandwidth between 85 to 120 GHz, which from Figure 10 is shown to be in close agreement with the measured NRW method.

TABLE 3.—RESULTS SUMMARY WITH RESONANT FREQUENCY (NO LOAD), FREE SPACE WAVELENGTH, CORRESPONDING α AND EXTRACTED REFRACTIVE INDEX

Sample number, thickness	f_0, GHz	λ_0, m	α	n
S_1 1.5 mm	86.64	0.00346	5	5.77
S_2 1.5 mm	103.97	0.00288	6	5.76
S_1 2.0 mm	89.45	0.00335	7	5.86
S_2 2.0 mm	102.17	0.00293	8	5.86
S_3 2.0 mm	114.99	0.00261	9	5.87
S_1 3.0 mm	86.30	0.00347	10	5.78
S_2 3.0 mm	95.08	0.00315	11	5.78
S_3 3.0 mm	103.74	0.00289	12	5.78
S_4 3.0 mm	112.35	0.00267	13	5.79

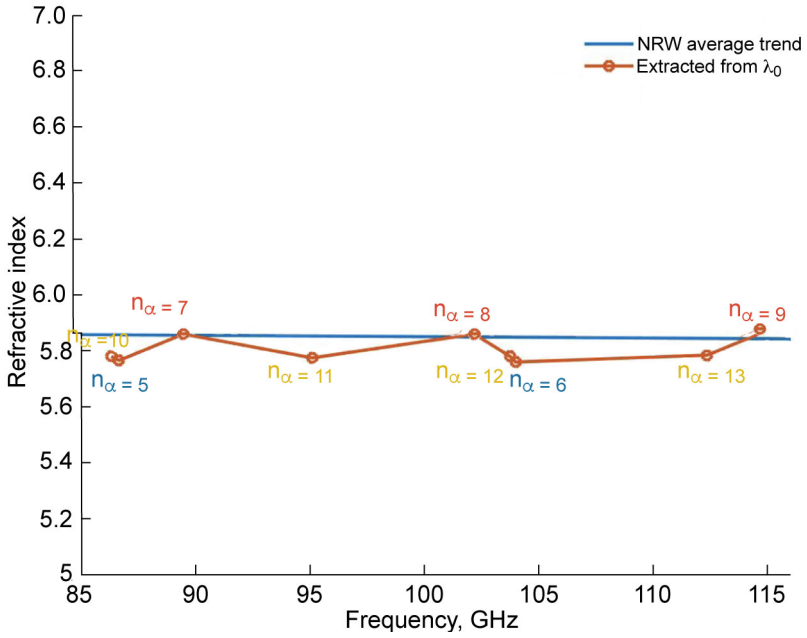

Figure 10.—Plot of extracted refractive index measurements of bulk YTZP using resonant wavelength approach along with refractive index measurements using NRW mu = 1 method in bandwidth of 85 to 120 GHz.

5.0 Discussion

The results of these experiments have been analyzed in terms of repeatability and accuracy which is dependent on the material properties and sensitivity of the measurement acquisition. The results showed consistent repeatability across varying calibrations, across samples specimens, and repeatability over multiple stress loading cycles. The material properties of YTZP are such that this in-situ measurement approach produces consistent and accurate results.

The resonant wavelength approach for analysis of refractive index is achievable when one can acquire numerous analysis points. The point frequency is dependent on substrate dielectric properties and material thickness. YTZP being such a high dielectric substrate with short effective wavelengths allows for a multitude of resonant wavelength points within a single sample thickness. This allowed for the acquisition of nine resonant wavelength points from three sample thicknesses which provides an accurate approximation of the refractive index of bulk YTZP across the entire 85 to 120 GHz bandwidth.

6.0 Conclusion

This paper describes a new method employed to analyze stress in bulk YTZP using a resonant wavelength approach that analyzes S-parameter measurements acquired in a quasi-optical free space setup. An average stress-optic coefficient value of $C = 1.42\times10^{-4} \pm 6.65\times10^{-6}$ (1/GPa) for bulk YTZP was measured in the range of 80 to 100 GHz. This resonant wavelength approach which calculates stress as is relates to reflected S-parameters allows for acquisition of a material's general stress-optic coefficient independent of sample thickness.

In addition, this paper describes how the resonant wavelength approach can be used to approximate the refractive index of a material. For the first time a refractive index of $n = 5.80 \pm 0.043$ was measured across the 85 to 115 GHz bandwidth for bulk YTZP using this technique. It has also been shown that the extraction of these material properties is independent of the resonant frequency point used for analysis.

Measurements of multiple samples for multiple cycles, taken at various calibration settings, showed the error in this measurement technique to be < 1 percent. This resonant wavelength approach is shown to be a viable nondestructive testing technique for the determination of stress induced birefringence in YTZP. This accuracy demonstration paves the way towards future in-situ experimental setup development for real world methods of TBC lifetime estimation.

References

1. R. Stevens, 1986. Introduction to Zirconia. Magnesium Elektron Publication No 113.
2. S. Sampaht, U. Schulz, M.O. Jarligo, and S. Kuroda, "Processing science of advanced thermal-barrier systems," MRS Bull. 37(10), 903–910 (2012).
3. R. Darolia, "Thermal barrier coatings technology: critical review, progress update, remaining challenges and prospects," Int. Mater. Rev. 58(6), 315–348 (2013).
4. P. Schemmel, G. Diederich, and A.J. Moore, "Measurement of direct strain optic coefficient of YSZ thermal barrier coatings at GHz frequencies," Opt. Express 25, 19968–19980 (2017).
5. Schemmel, Peter J.: Reducing Aviation Fuel Costs With Non-Destructive Testing. NASA/TM—2019-220165, 2019. http://ntrs.nasa.gov
6. P. Schemmel, G. Deiderich, and A.'J. Moore, "Direct stress optic coefficients for YTZP ceramic and PTFE at GHz frequencies," Opt. Express 24, 8110–8119 (2016).
7. Schemmel, Peter J. Waldstein, Seth W: Microwave Photoelasticity: A resonant Wavelength Approach Applied to Peek Polyemer. NASA/TM—2020-220499, 2020. http://ntrs.nasa.gov
8. B. Maffei, S. Legg, M. Robinson, F. Ozturk, M.W., Ng, P. Schemmel, and G. Pisano, "Implementation of a quasi-optical free-space s-parameter measurement system," in Proceedings of the 35th ESA Antenna Workshop on Antenna and Free Space RF Measurements, 10–13 September (2013), ESTEC, Noordwijk, The Netherlands.
9. Nicolson A.M., Ross G.F., Measurement of the intrinsic properties of materials by time-domain techniques. IEEE Transactions on Instrumentation and Measurement. 1970; 19:377-382. DOI: 10.1109/TIM.1970.4313932.